

# Finite surface method to measure the sound absorption coefficient at oblique incidence

Marco Ottink<sup>1</sup>, Jonas Brunskog<sup>2</sup>, Cheol-Ho Jeong<sup>2</sup>, Efrén Fernandez Grande<sup>2</sup>,  
Elisabet Tiana Roig<sup>2</sup>, Per Trojgaard<sup>3</sup>

<sup>1</sup> Müller-BBM GmbH, Hamburg, Germany, Email: Marco.Ottink@mbbm.com

<sup>2</sup> Acoustic Technology, DTU Electrical Engineering, Technical University of Denmark, Denmark

<sup>3</sup> Lloyds Register Consulting - Engineering Dynamics, Denmark

## Introduction

Common methods to estimate the sound absorption coefficient are the chamber method (for random incidence)<sup>2</sup> and a method based on Impedance tube measurements (for normal incidence).<sup>1</sup> Besides these well accepted measurements, a method to measure the absorption coefficient depending on the angle of incidence is increasingly needed. So far studies regarding angle dependent measurements in free field conditions failed to compute the absorption coefficient for high incidence angles.<sup>5–8</sup> Even though measurements were carried out with a finite absorber sample, these methods are based on the theory of an infinite sample size. It was found that the finiteness of the absorber has a significant influence on the measured absorption coefficient for high incident angles, as e.g., shown by Thomasson.<sup>3,4</sup>

The goal of the present study is to measure the angle dependent absorption coefficient by taking the finiteness of the sample into account using an inverse finite surface method. This method aims to estimate the impedance of the absorber in an inverse measurement approach. Therefore Thomasson's theory is extended to predict the sound field in front of a finite sized absorber placed on a rigid backing.

For validation three in-situ methods are used: the temporal subtraction method, the microphone array method, and the finite surface method.

## Theory

The time convention  $e^{j\omega t}$  is used, where  $\omega = 2\pi f$  is the angular frequency and  $t$  is the time. Furthermore, the surface impedance  $Z_A$ , normalized by  $\rho c$ , is used, where  $c$  is the speed of sound and  $\rho$  is the density of air.

### Sound field model

The presented sound field model, which considers scattering from the finite absorber, is derived from the methods described by Thomason<sup>3,4</sup> and Morse and Ingard.<sup>12</sup>

The sound field model is based on an incident plane wave and a specular plane wave, as shown in Fig. 1. The absorber with arbitrary surface area  $S$  and admittance  $\beta = 1/Z_A$  is placed on a surface with admittance  $\beta_0$ . The pressure amplitudes of the reflected and incident plane waves are considered to be equal, similar to the reflection on a rigid baffle. Scattering from the surrounding baffle and the absorber are considered separately. The sound pressure at point  $P \in (x, y, z)$ , by considering an incident plane wave and scattering from the surface, can

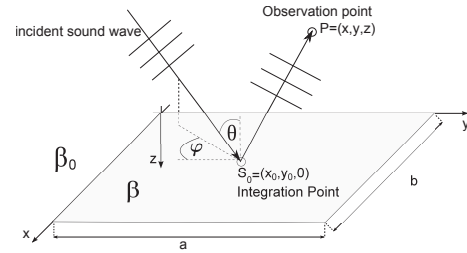


**Figure 1:** Sketch illustrating the sound field model considering the finiteness of the absorber

be described as an integral equation,<sup>12</sup>

$$p(x, y, z) = \hat{p}_i \left( e^{-j(k_x x + k_y y + k_z z)} + e^{-j(k_x x + k_y y - k_z z)} \right) + jk\Delta\beta \int_S G(x, y, z|x_0, y_0, 0) p(x_0, y_0, 0) dS_0, \quad (1)$$

where  $k_x = k \sin \theta \cos \varphi$ ,  $k_y = k \sin \theta \sin \varphi$ , and  $k_z = k \cos \theta$  are the wave numbers, expressed in terms of the incidence angle  $\theta$  and the azimuth angle  $\varphi$ , where  $k = \omega/c$  is the wave number in air,  $\Delta\beta = \beta - \beta_0$  is the change of admittance between the absorber and the surrounding baffle,  $p(x_0, y_0, 0)$  is the pressure function on the absorber surface at  $z = 0$ ,  $\int_S dS_0$  is the integral over the material surface and  $G(x, y, z|x_0, y_0, 0) = e^{-jk_d}/(2\pi d)$  is the half space Green's function between the respect integration point  $S_0 \in (x_0, y_0, 0)$  and the observation point  $P$ . The distance  $d$  between the observation point  $P$  and the surface point  $S_0$  is given by  $d = \sqrt{(x - x_0)^2 + (y - y_0)^2 + z^2}$ .

Here, the finite absorber is surrounded by an infinite rigid baffle ( $\beta_0 = 0$ ). Thus  $Z_A$  represents the surface impedance of the absorbing material. The unknown sound pressure  $p$  in the integral equation, Eq. (1), cannot be solved explicitly. Thus the solution of the integral equation is found by using a variational principle, shown in Refs. 3, 4 and 11 - 13, as

$$p(x, y, z) = \hat{p}_i \left( e^{-j(k_x x + k_y y + k_z z)} + e^{-j(k_x x + k_y y - k_z z)} \right) + \hat{p}_i \left( \frac{2jkF(x, y, z|x_0, y_0)}{Z_A + Z_F} \right), \quad (2)$$

where

$$F(x, y, z|x_0, y_0) = \int_S G(x, y, z|x_0, y_0, 0) e^{-j(k_x x_0 + k_y y_0)} dS_0,$$

and  $Z_F$  is the normalized specific radiation impedance, as defined by Thomasson<sup>3</sup>.

### Computation of the radiation impedance

The radiation impedance can be fully determined by size and geometry of the absorber, as shown in Refs. 3 and 4. For large Helmholtz numbers, the surface impedance  $Z_F$  approaches  $1/\cos\theta$ , similar to the assumption of plane wave reflections from an infinite absorber sample. For small Helmholtz numbers  $ke$  this assumption is just a good approximation for small incidence angle, near grazing incidence this does not hold anymore.

However, the computation of Thomasson's formulation for a rectangular absorber is not well suited for numerical integration. A more convenient expression, based on a variable substitution, is used in this study as<sup>14</sup>

$$Z_F = -\frac{jk}{2\pi S} \int_0^a \int_0^b 4 \cos(k_x \kappa) \cos(k_y \tau) \frac{e^{-jk\sqrt{\kappa^2 + \tau^2}}}{\sqrt{\kappa^2 + \tau^2}} (a - \kappa)(b - \tau) d\kappa d\tau. \quad (3)$$

### Computation of the absorption coefficient

It is well known that the measured absorption coefficient according to ISO 354<sup>2</sup> can exceed unity due to the dependency on the absorber area. Therefore, the angle dependent absorption coefficient  $\alpha(\theta)$  for finite absorbers is determined from the radiation impedance  $Z_F$  and the surface impedance  $Z_A$  by using Thomasson's alternative absorption coefficient<sup>4</sup> as

$$\alpha(\theta) = \frac{4\Re\{Z_A\}\Re\{Z_F\}}{|Z_A Z_F|^2} \quad (4)$$

In case of assuming an infinite absorber sample,  $Z_F = 1/\cos(\theta)$ , the ordinary definition of the absorption coefficient is used<sup>16</sup> as

$$\alpha_\infty(\theta) = 1 - \left| \frac{Z_A - \frac{1}{\cos(\theta)}}{Z_A + \frac{1}{\cos(\theta)}} \right|^2, \quad (5)$$

$$= 1 - |R(\theta)|^2, \quad (6)$$

where  $R(\theta) = \frac{\hat{p}_r}{\hat{p}_i}$  is the reflection factor, and  $\hat{p}_i$  and  $\hat{p}_r$  are the complex pressure amplitudes of the incident to reflected plane waves, respectively.<sup>8-11</sup>

### In-situ measurement methods

Three in-situ methods to measure the absorption coefficient are used. Besides the well accepted *temporal subtraction method*<sup>6,7</sup> a *microphone array method* is used, both assuming an infinite absorber sample to estimate the absorption coefficient by using Eq. (5). Furthermore a *finite surface method* is proposed, which takes into account the finiteness of the absorber using an inverse technique. The finite surface method estimates the surface impedance  $Z_A$  to calculate the absorption coefficient  $\alpha$  with Eq. (4). A sketch of the measurement methods is shown in Fig. 2.

#### Temporal subtraction method

The temporal subtraction method is based on impulse response measurements above the surface under test, by

using a single microphone. For post-processing, a subtraction method as in Refs. 6 and 7 is used. Therefore, another impulse response, without the absorbing material, is measured by keeping the loudspeaker microphone distance constant.

#### Microphone array method

The microphone array method is based on sound pressure measurements with an array of microphones. The statistically optimized near-field acoustic holography (SONAH)<sup>21</sup> is used to estimate the incident and reflected sound pressure in a reconstruction plane  $z_s$  based on measurements in two horizontal planes,  $z_{h1}$  and  $z_{h2}$ , above the absorber. Details about SONAH are shown in Refs. 18-20. The respective coefficients in SONAH are solved in a Least-Squares sense, and using Tikhonov regularization.<sup>22</sup> A detailed description of this procedure is shown in Ref. 19.

The reflection factor for the  $n^{\text{th}}$  microphone in the reconstruction plane is calculated as the quotient of the estimated reflected and incident sound pressure close to the absorber. The overall reflection factor  $|R|$  is calculated as the average value of all  $|R_n|$ .

#### Finite surface method

To estimate the surface impedance for oblique sound incidence, the finite surface method combines the sound field model with microphone array measurements in an inverse manner.

Since the measurements are performed with  $N$  microphones at discrete positions, the sound pressure amplitude  $\hat{p}_i$  is estimated by minimizing the least-squares principle

$$E_{LS}(\hat{p}_i) \simeq \sum_{n=1}^N |\hat{p}_i e^{-j(k_x x_{0,n} + k_y y_{0,n} + k_z z_{0,n})} - p_i(x_{0,n}, y_{0,n}, z_{0,n})|^2, \quad (7)$$

where  $p_i(x_{0,n}, y_{0,n}, z_{0,n})$  is the estimated incident sound pressure at position  $n$  obtained with SONAH using the microphone array method and  $\hat{p}_i e^{-j(k_x x_{0,n} + k_y y_{0,n} + k_z z_{0,n})}$  is the incident sound pressure at position  $n$ , where  $\hat{p}_i$  is the incident pressure amplitude.

By using the estimated incident sound pressure amplitude from Eq. (7), the surface impedance is determined by minimizing the least-square principle

$$E_{LS}(Z_A) \simeq \sum_{n=1}^N |p_{fw,n}(x, y, z|Z_A) - p_{t,n}(x, y, z)|^2, \quad (8)$$

where  $p_{t,n}(x, y, z)$  is the total measured sound pressure at each position in the measurement plane and  $p_{fw,n}(x_n, y_n, z_n|Z_A)$  is the forward model sound pressure based on Eq. (2).

The cost functions are minimized using simplex optimization, by the use of the Matlab function *fminsearch*. Here the initial guesses are the mean incident sound pressure amplitude over all reconstruction positions and the surface impedance estimated from an equivalent fluid model, Miki model<sup>24</sup>, by using the radiation impedance for finite absorbers.

## Measurement setup

All measurements are performed in a large anechoic chamber at DTU with a low frequency limit of about 50 Hz. The absorber under test is the "Industrial" absorber from Rockfon,<sup>25</sup> with thickness of  $h_d = 5$  cm and flow resistivity of  $1.42 \cdot 10^4$  Ns/m<sup>4</sup>, measured with the impedance tube method, described by Ren and Jacobsen.<sup>26</sup>

A large and heavy squared wooden plate of 3 cm thickness and area of about 14 m<sup>2</sup> is placed in the anechoic chamber to approximate the rigid and infinite backing, on which the square sized absorber, with a side length of 1.2 m, is placed centered, see Fig. 2.

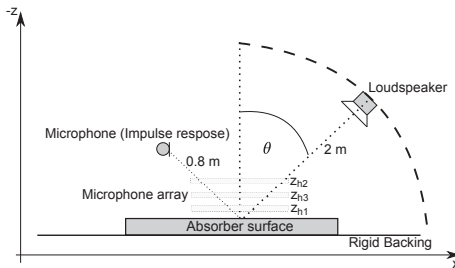


**Figure 2:** Sketch illustrating the three measurement setups.

The measurements are performed with an omni directional source<sup>27</sup> at incident angles  $\theta = \{0^\circ, 45^\circ, 60^\circ, 85^\circ\}$ . The distance between the absorber center and the source is kept constant at 2 m. The distance between absorber center and the microphone (temporal subtraction method) is kept constant at 0.8 m and with respect to the incident angle. The planar array with 60 pressure microphones (microphone array and finite surface method) is placed at three horizontal  $x$ - $y$  planes,  $z_{h1} = 4$  cm,  $z_{h2} = 8$  cm,  $z_{h3} = 6$  cm (for the SONAH reconstruction just  $z_{h1}$  and  $z_{h2}$  are used). Since the error of the SONAH reconstruction increases at the edges of the array, only the 24 center reconstruction positions are used for estimation of the sound pressure amplitudes. For the forward model, measurements in three parallel planes (180 measurement points) are considered. To validate the experiments, impedance tube measurements at normal incidence are performed. Furthermore, for validation against theory, an equivalent fluid model, Miki model, is used.<sup>24</sup> The surface impedance  $Z_A$  at oblique incidence  $\theta$  for an absorber placed on a rigid and infinite backing is calculated by using a plane wave assumption.<sup>10</sup> The equivalent fluid model is used with two different radiation impedances  $Z_F$ , based on an infinite sample,  $Z_F = 1/\cos(\theta)$ , and a finite sample, Eq. (3). The corresponding absorption coefficient is either calculated with Eq. (4) (finite sample) or with Eq. (5) (infinite sample).

## Measurement results

The results are given in Fig. 3, with incidence angles of  $\theta = \{0^\circ, 45^\circ, 60^\circ, 85^\circ\}$ .

### Equivalent fluid model

Fig. 3(a) shows a good agreement between the impedance-tube measurement and the theory at normal incidence.

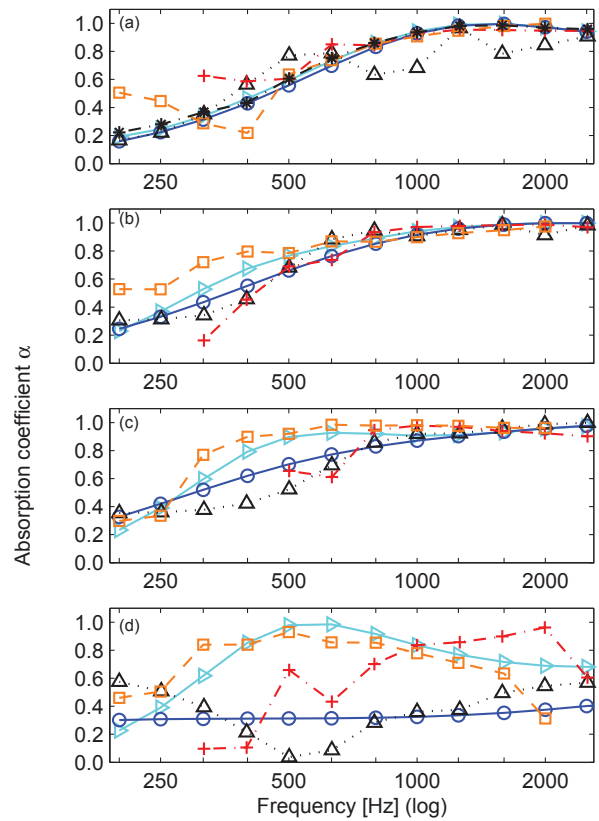


**Figure 3:** Absorption coefficient of a sample with a side length of 1.2 m. (a):  $\theta = 0^\circ$ , (b):  $\theta = 45^\circ$ , (c):  $\theta = 60^\circ$ , (d):  $\theta = 85^\circ$ , (-o) Miki model:  $Z_F$  of an infinite sample, (-▷) Miki model:  $Z_F$  of a finite sample, (-·-\*) Impedance tube, (··△) Temporal subtraction method, (-·-+) Microphone array method, (-·-□) Finite surface method.

Furthermore, for normal incidence, the equivalent fluid model using the radiation impedance of a finite sample and the radiation impedance of an infinite sample are very similar. With increasing incidence angle, shown in Fig. 3(b-d), the calculated absorption coefficient assuming an infinitely absorber sample decreases and approaches zero at grazing incidence, while the absorption coefficient using the radiation impedance of a finite sample still shows a high absorption.

### Temporal subtraction and microphone array method

Figure 3 shows that it is difficult to get sufficiently accurate results even for small incident angles using the temporal subtraction method and the microphone array method. In the temporal subtraction method a detailed post processing is used. Nevertheless, the time difference between the directly reflected part and the diffracted reflected part of the impulse response becomes too small to obtain accurate results. The microphone array method agrees well with the theory at normal incidence for frequencies above 400 Hz. With increasing incidence angle the results increasingly deviate from theory. Both methods assume the plane wave reflection to calculate the absorption coefficient.

The deviations from theory for  $\theta > 45^\circ$  show, that for finite and small absorbers an advanced method that accounts for the absorber finiteness is needed.

## Finite surface method

Figure 3(d) shows, that especially near grazing incidence (here  $\theta = 85^\circ$ ), the finite surface method gives a promising agreement with the theory by using the finite surface radiation impedance between 200 Hz and 1.5 kHz approximately. A similar result is found for an incident angle of  $60^\circ$ , Fig 3(c).

Figure 3(b-c) shows, that for small incident angles a good agreement with the theory is found for frequencies above 200 Hz. At normal incidence, Fig. 3(a), the results from the finite surface method deviate from the theory for frequencies below 500 Hz. This could be explained by the fact that for small differences in the measurement planes the phase differences between two consecutive microphones become very small, thus capturing very similar phase.<sup>19</sup>

## Conclusions

Three different measurement methods to measure the acoustic property of finite sound absorbers at oblique incidence are proposed: the well accepted temporal subtraction method, the microphone array method and the proposed finite surface method. With the finite surface method the finiteness of the absorber is taken into account by using an inverse method with a sound field model for finite absorbers considering scattering reflections. Good agreement between the proposed finite surface method and the equivalent fluid model is found, especially for nearly grazing incidence and a small specimen. For future measurements better results for lower frequencies are expected by carefully choosing a microphone grid with greater distances between the measurement planes and advanced post-processing. In conclusion the finite surface method can be used for measuring the oblique incidence absorption coefficient for finite absorbers.

## References

- [1] ISO 10534-2, *Acoustics - Determination of sound absorption coefficient and impedance in impedance tubes - Part 2: Transfer-function method*, (International Organization for Standardization, Geneva, 1998).
- [2] ISO 354, *Acoustics - Measurement of sound absorption in a reverberation room*, (International Organization for Standardization, Geneva, 2003).
- [3] S.-I. Thomasson, *On the absorption coefficient*, (Acta Acustica united with Acustica **44**(4) 265–273 1980).
- [4] S.-I. Thomasson, *Theory and experiments on the sound absorption as function of the area*, (Report, TRITA-TAK-8201, KTH Stockholm, 1982).
- [5] U. Ingard, and R.-H. Bolt, *A free field method of measuring the absorption coefficient of acoustic materials*, (J. Acoust. Soc. Am. **23**(5), 509–516, 1951).
- [6] E. Mommertz, *Angle-dependent in-situ measurements of reflection coefficients using a subtraction technique*, (Applied Acoustics **46**, 251–263, 1995).
- [7] P. Robinson, and N. Xiang, *On the subtraction method for in-situ reflection and diffusion coefficient measurements*, (J. Acoust. Soc. Am. Express Letters **127** (3), EL99–EL104, March 2010).
- [8] K. Hirose, H. Nakagawa, M. Kon, and A. Yamamoto, *Comparison of three measurement techniques for the normal absorption coefficient of sound absorbing materials in the free field*, (J. Acoust. Soc. Am. **126** (6), 3020–3027, 2009).
- [9] F.-P. Mechel, *On sound absorption of finite-size absorbers in relation to other radiation impedances*, (Journal of Sound and Vibration **135** (2), 225–262, 1989).
- [10] J.-S. Pyett, *The acoustic impedance of a porous layer at oblique incidence*, (Acta Acustica **3** 375–382, 1953).
- [11] F.-P. Mechel, *Schallabsorber - Band 1, Äußere Schallfelder, Wechselwirkungen* (English translation: Sound absorbers - Part 1, external sound fields, interactions), (Hinzel Verlag, Stuttgart 39–51, 232–276, 1989).
- [12] P.-M. Morse, and K.-U. Ingaard, *Theoretical acoustics*, (Princeton university press, Princeton , 155–163, 1968).
- [13] J. Brunskog, and P. Hammer, *Rigid indenter excitation of plates*, (Acta Acust. Acust. **89**, 460–470, 2003).
- [14] J. Brunskog, *Forced sound transmission of finite single leaf walls using a variational technique*, (J. Acous. Soc. Am. **132** (3), 1482–1493, 2012).
- [15] J.-L. Davy, et al. *The average specific forced radiation wave impedance of a finite rectangular panel*, (J. Acoust. Soc. Am. **136**, 525–536, 2014).
- [16] E.-T. Paris, *On the coefficient of sound-absorption measured by the reverberation method*, (Philos. Mag. **5** 489–497, 1928).
- [17] ISO 13472-1, *Acoustics - Measurement of sound absorption properties of road surfaces in situ - Part 1: Extended surface method*, (ICS **17.140.30**; **93.080.20**, 2012).
- [18] E. Fernandez-Grande, *Near-field acoustic holography with sound pressure and particle velocity measurements*, (PHD thesis at the Technical University of Denmark (DTU) , 2012).
- [19] E. Fernandez-Grande, F. Jacobsen, and Q. Leclere, *Sound field separation with sound pressure and particle velocity measurements*, (J. Acous. Soc. Am. **132** (6) 3818–3825, 2012).
- [20] J.-D. Maynard, E.-G. Williams, and Y. Lee, *Nearfield acoustic holography: Theory of generalized holography and the development of NAH*, (J. Acous. Soc. Am. **78** (4) 1395–1413, 1985).
- [21] J. Hald, *Basic theory and properties of statistically optimized near-field acoustical holography*, (J. Acous. Soc. Am. **125** 2105–2120, 2009).
- [22] P.-C. Hansen, *Analysis of discrete ill-posed problems*, (Soc. for Industrial and Applied Mathematics, SIAM Philadelphia , 1992).
- [23] J.-A. Nelder, and R. Mead, *A simplex-method for function minimization*, (Computer Journal **7** (4) 308–313, 1965).
- [24] Y. Miki, *Acoustical properties of porous materials - modification of Delany-Bazley models*, (Journal of the Acoustic Society of Japan **11** 19–24, 1990).
- [25] Rockfon, *Rockfon Industrial Opal/Black/Nature*, (Product catalog from Rockfon: [http://products.exp-en.rockfon.com/media/286660/datasheet\\_exp\\_industrial\\_02.2011.pdf](http://products.exp-en.rockfon.com/media/286660/datasheet_exp_industrial_02.2011.pdf) (date last viewed 02/13/2015)).
- [26] M. Ren, and F. Jacobsen, *A method of measuring the dynamic flow resistance and reactance of porous materials*, (Applied Acoustics, **39**(4), 265–276, 1993).
- [27] L.-R. Fincham, A. Jones, and R.-H. Small, *The influence of room acoustics on reproduced sound, Part 2: Design of wide-band coincident-source loudspeakers*, (Audio Engineering Society **87**, 1989).
- [28] M.-E. Delany, and E.-N. Bazley, *Acoustical characteristics of fibrous absorbent materials*, (Applied Acoustics **3** 105–116, 1970).